A postsynaptic Spectrin scaffold defines active zone size, spacing, and efficacy at the *Drosophila* neuromuscular junction

Jan Pielage,[1,2] Richard D. Fetter,[1,2] and Graeme W. Davis[1,2]

[1]Department of Biochemistry and Biophysics and [2]Program in Neuroscience, University of California, San Francisco, San Francisco, CA 94143

Synaptic connections are established with characteristic, cell type–specific size and spacing. In this study, we document a role for the postsynaptic Spectrin skeleton in this process. We use transgenic double-stranded RNA to selectively eliminate α-Spectrin, β-Spectrin, or Ankyrin. In the absence of postsynaptic α- or β-Spectrin, active zone size is increased and spacing is perturbed. In addition, subsynaptic muscle membranes are significantly altered. However, despite these changes, the subdivision of the synapse into active zone and periactive zone domains remains intact, both pre- and postsynaptically. Functionally, altered active zone dimensions correlate with an increase in quantal size without a change in presynaptic vesicle size. Mechanistically, β-Spectrin is required for the localization of α-Spectrin and Ankyrin to the postsynaptic membrane. Although Ankyrin is not required for the localization of the Spectrin skeleton to the neuromuscular junction, it contributes to Spectrin-mediated synapse development. We propose a model in which a postsynaptic Spectrin–actin lattice acts as an organizing scaffold upon which pre- and postsynaptic development are arranged.

Introduction

Synapses are specialized intercellular junctions that are required for the transfer of information between neurons. At chemical synapses, the presynaptic neuron forms a specialized membrane domain, termed the active zone, which contains the molecular machinery required for calcium-dependent synaptic vesicle fusion and recycling. A postsynaptic density, consisting of concentrated neurotransmitter receptors, forms in direct apposition to the active zone. A fundamental feature of chemical synapses is that they can be modulated to alter the transfer of information between neurons (Bredt and Nicoll, 2003). There are several general mechanisms by which the strength of synaptic connections can be influenced, including the following: (a) a change in the probability of synaptic vesicle fusion in response to a presynaptic action potential, (b) a change in the density or sensitivity of postsynaptic receptors, and (c) a change in synapse size (defined as the area of opposed presynaptic active zone membrane and postsynaptic density; Murthy et al., 2001). A strong correlation between synapse size and the probability of presynaptic release has lead to speculation that the regulation of synapse size could participate in the mechanisms of neural development and activity-dependent plasticity (Schikorski and Stevens, 1997). Although the mechanisms that modulate vesicle fusion and postsynaptic receptor trafficking have received considerable attention, little is known about the molecular mechanisms that control synapse size. In *Drosophila melanogaster* and *Caenorhabditis elegans*, genetic studies have uncovered several signaling molecules that, when mutated, affect synapse size. These signaling molecules include Liprin-α/Syd-2, Dlar, and Dally-like (Zhen and Jin, 1999; Kaufmann et al., 2002; Johnson et al., 2006). It remains to be determined how these signaling molecules mediate their influence on synapse size.

We investigate the role of the postsynaptic Spectrin skeleton in the regulation of synapse size. The Spectrin skeleton consists of heterotetramers of two α- and two β-Spectrin subunits that, together with short actin filaments, form a cytoplasmic Spectrin–actin network that parallels the plasma membrane. The Spectrin skeleton can be recruited to the plasma membrane in several ways, including interactions with the adaptor protein Ankyrin, direct interactions with integral membrane proteins, or through interactions with plasma membrane phospholipids (Bennett and Baines, 2001). In the vertebrate nervous system, Spectrin and Ankyrin are required for the organization of ion

Correspondence to Graeme W. Davis: gdavis@biochem.ucsf.edu

Abbreviations used in this paper: ds, double stranded; EPSP, excitatory postsynaptic potential; mepsp, miniature EPSP; NMJ, neuromuscular junction; Pak, p21-activated kinase; RNAi, RNA interference; SSR, subsynaptic recombination.

The online version of this article contains supplemental material.

The Journal of Cell Biology, Vol. 175, No. 3, November 6, 2006 491–503
http://www.jcb.org/cgi/doi/10.1083/jcb.200607036

channels and cell adhesion molecules into discrete domains. For example, at the nodes of Ranvier and at axon initial segments, Ankyrin G assembles a protein complex of voltage-gated sodium channels, L1-family cell adhesion molecules, and βIV-Spectrin. The organization of these membrane domains is severely impaired in *ankyrin G* and *βIV-spectrin* mutant mice, demonstrating that Ankyrin G and βIV-Spectrin mutually stabilize these integral membrane clusters (Jenkins and Bennett, 2001; Komada and Soriano, 2002; Ango et al., 2004; Lacas-Gervais et al., 2004). Spectrin is found at synaptic connections throughout the central and peripheral nervous system (Phillips et al., 2001) and has been hypothesized to participate in the clustering of postsynaptic neurotransmitter receptors (Bloch and Morrow, 1989; Wechsler and Teichberg, 1998). However, direct genetic evidence documenting such a role for Spectrin is lacking.

In *C. elegans*, Spectrin is required for neuronal outgrowth and sarcomere stabilization in muscle. Interestingly, an ultrastructural analysis did not reveal obvious defects at the neuromuscular junction (NMJ; Hammarlund et al., 2000; Moorthy et al., 2000). In *D. melanogaster*, α- and β-Spectrin are present at the NMJ and null mutations in *α-spectrin* or *β-spectrin* die at the late embryonic/early larval stages (Lee et al., 1993; Dubreuil et al., 2000; Featherstone et al., 2001; Pielage et al., 2005). In *spectrin*-null mutant embryos, synaptogenesis proceeds, but synaptic efficacy is impaired and the localization of both presynaptic vesicle proteins and postsynaptic Discs-large (PSD-95 homologue) is altered. Despite these defects in protein localization, iontophoretic application of glutamate evoked normal postsynaptic currents, suggesting that glutamate receptors are normally recruited to the nascent embryonic NMJ in the absence of α- or β-Spectrin (Featherstone et al., 2001). Embryonic lethality precluded further analysis of synapse maturation and stability.

To analyze the function of α- and β-Spectrin during postembryonic synapse development, we have previously used a transgenic RNA interference (RNAi) approach that allows us to circumvent the embryonic lethality associated with *α-* and *β-spectrin* mutations. We demonstrated that we can efficiently knock down α- or β-Spectrin at either the pre- or the postsynaptic side of the larval NMJ, and that the presynaptic Spectrin skeleton is essential for the stability of the NMJ (Pielage et al., 2005). We document a separable and unique requirement of the postsynaptic Spectrin skeleton for the specification of active zone size, spacing, and function during postembryonic development. We then extend our observations to include an analysis of postsynaptic Ankyrin, demonstrating that Ankyrin participates in the Spectrin-dependent regulation of synapse development. Together, our data suggest the existence of a postsynaptic, submembranous Spectrin–actin network that imposes a transsynaptic organization upon synapse development at the *D. melanogaster* NMJ.

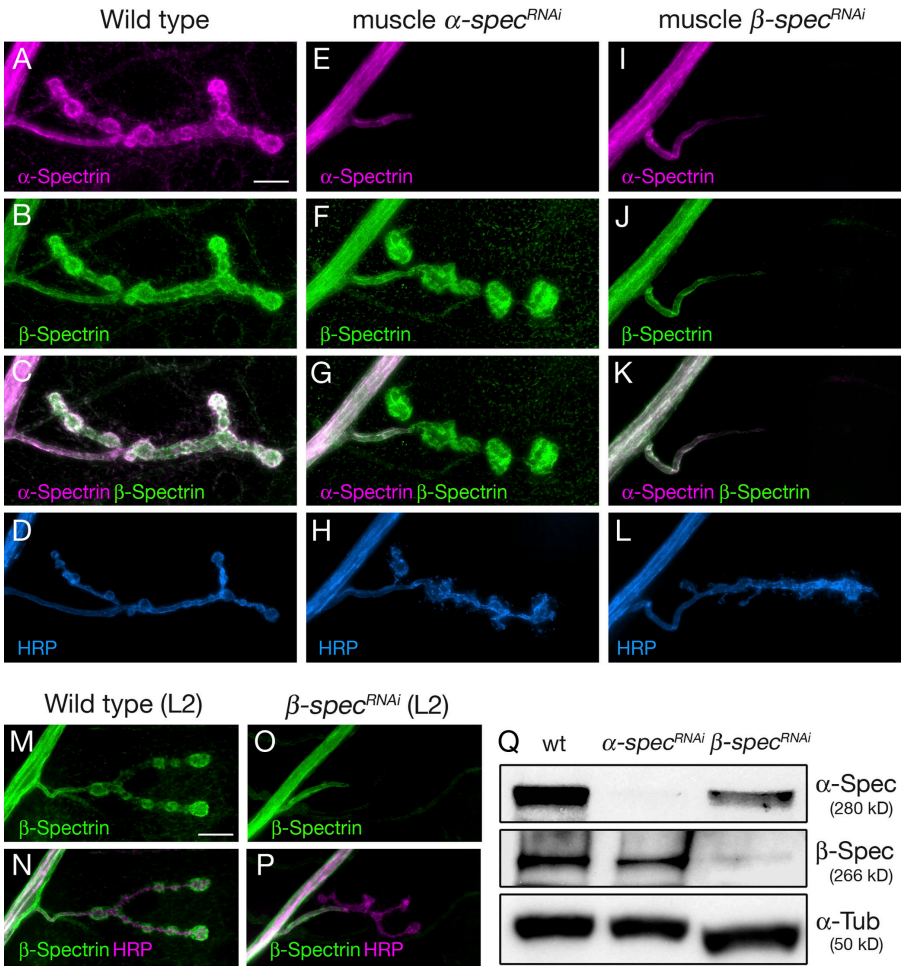

Figure 1. **Postsynaptic elimination of α- and β-Spectrin at the NMJ.** (A–D) A third instar wild-type synapse at muscle 4 is stained for α-Spectrin (A), β-Spectrin (B), and the presynaptic membrane marker HRP (D). α- and β-Spectrin colocalize and are highly enriched in the postsynaptic SSR (C). (E–H) Muscle-specific expression of *α-spectrin* dsRNA leads to the elimination of α-Spectrin in the muscle, but not in the motoneuron axon (E). β-Spectrin protein levels in the muscle are unchanged, but the distribution of β-Spectrin within the SSR is severely affected (F and G). (I–L) Muscle-specific expression of *β-spectrin* dsRNA results in the elimination of β- and α-Spectrin from the postsynaptic muscle (I–K). The presynaptic nerve terminal can be identified by HRP (L). A second instar wild-type synapse is shown stained for β-Spectrin (M and N) and HRP (N). (O and P) Expression of *β-spectrin* dsRNA results in the elimination of β-Spectrin from the muscle in second instar larvae. (Q) Western blot analysis of third instar larvae. The ubiquitous expression of *α-spectrin* dsRNA results in the elimination of α-Spectrin, but not β-Spectrin protein levels. The ubiquitous expression of *β-spectrin* dsRNA greatly reduces β-Spectrin protein, with only minor effects on α-Spectrin protein levels. Bars, (A–P) 10 μm.

Results

We first confirm our ability to knock down Spectrin protein by expressing *spectrin* double-stranded RNA (dsRNA) in muscle, beginning in the first larval instar stage (Fig. 1, E and J; see Materials and methods). Interestingly, the expression of *β-spectrin* dsRNA eliminates both β- and α-Spectrin protein from the postsynaptic muscle membrane (Fig. 1, I–L), whereas the expression of *α-spectrin* dsRNA eliminates only α-Spectrin protein (Fig. 1, E–H). We tested the specificity of our dsRNA constructs and show that ubiquitous *α-spectrin* dsRNA expression knocks down α-Spectrin protein without substantially affecting β-Spectrin protein levels (Fig. 1 Q). Similarly, *β-spectrin* dsRNA expression strongly reduces β-Spectrin protein levels, with only minor effects on α-Spectrin protein levels (Fig. 1 Q). These experiments demonstrate that transgenically expressed dsRNA can knock down α- or β-Spectrin protein in the muscle below levels detectable by light microscopy. We conclude that β-Spectrin is required for the localization and/or stabilization of α-Spectrin to the postsynaptic muscle membrane, as has been observed in other *D. melanogaster* tissues (Dubreuil et al., 2000).

We next tested the time required for Spectrin protein knockdown after dsRNA expression in the muscle. We find that β-Spectrin protein is eliminated from larval muscle by the second instar stage, ∼24 h after the onset of *β-spectrin* dsRNA expression (Fig. 1, O and P). An identical result is observed for α-Spectrin (unpublished data). Because we conduct our assays in wandering third instar larvae, we estimate that the NMJ has developed in the near absence of postsynaptic α- or β-Spectrin for at least 3 d.

Postsynaptic Spectrin is necessary for synaptic growth

To assay the function of postsynaptic α- or β-Spectrin during synapse development we stained NMJs with the presynaptic vesicle marker synaptotagmin (Syt) and the postsynaptic subsynaptic reticulum (SSR) marker Discs-large (Dlg; Fig. 2, A–C). This combination of synaptic markers enables us to analyze NMJ stability, growth, and morphology (Eaton et al., 2002; Eaton and Davis, 2005; Pielage et al., 2005). In the absence of postsynaptic α- or β-Spectrin, the postsynaptic membrane markers are severely perturbed (Fig. 2, B and C). However, markers for the presynaptic nerve terminal always remain at the NMJ within the synaptic domain defined by markers for the SSR (Fig. 2, B and C) and in direct opposition to postsynaptic glutamate receptors (see below). Thus, although the postsynaptic membranes are perturbed, we can conclude that the stability of the presynaptic nerve terminal has not been impaired after the loss of postsynaptic Spectrin (Pielage et al., 2005).

Because postsynaptic organization is severely perturbed, we quantified synaptic bouton number at the NMJ as a measure of NMJ growth. Bouton number is significantly reduced in animals lacking either α- or β-Spectrin, demonstrating that postsynaptic Spectrin is necessary for normal NMJ growth (Fig. 2 D). Interestingly, this NMJ growth phenotype is more severe in animals lacking postsynaptic β-Spectrin compared with animals lacking postsynaptic α-Spectrin (Fig. 2 D). Because β-Spectrin remains at the postsynaptic SSR in animals lacking postsynaptic α-Spectrin (Fig. 1 F), these differential effects might reflect a function of β-Spectrin that persists in the absence of postsynaptic α-Spectrin.

Postsynaptic Spectrin is necessary for the formation of subsynaptic muscle membrane folds

The most striking phenotype at NMJs that lack either postsynaptic α- or β-Spectrin is the disruption of the SSR. At the light level, the SSR can be visualized by antibody staining for Dlg,

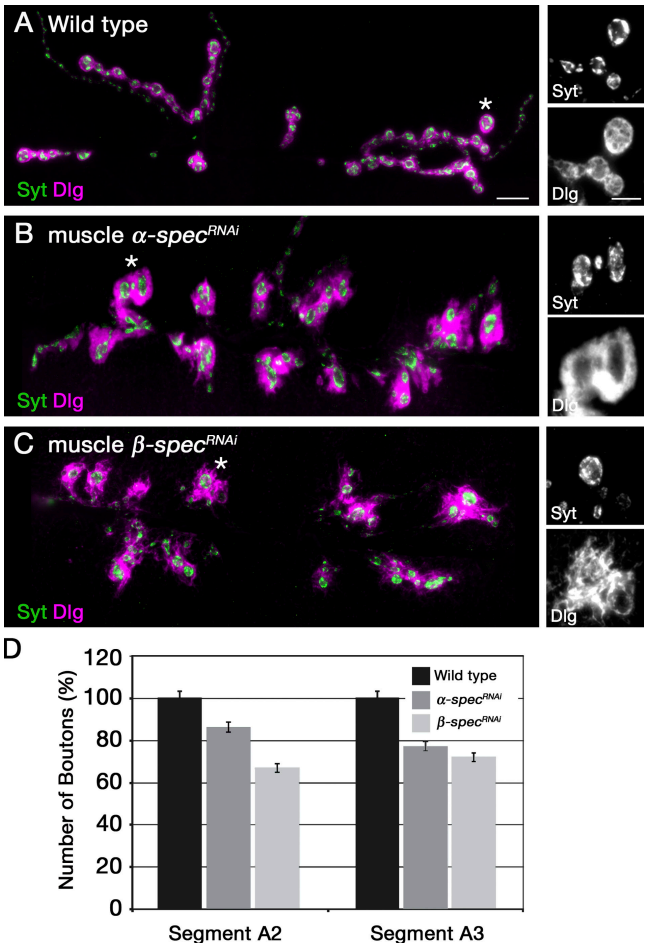

Figure 2. **Loss of postsynaptic α- or β-Spectrin results in severe morphological defects in NMJ formation.** (A–C) NMJs from muscle 6 and 7 at segment A3 are shown stained for the presynaptic vesicle marker synaptotagmin (Syt; green) and for the postsynaptic SSR marker Discs-large (Dlg; magenta). (right) Higher resolution images of areas indicated by asterisks. (A) In wild type, the postsynaptic marker Dlg tightly surrounds the presynaptic nerve terminal marked by Syt. (B) A NMJ lacking postsynaptic α-Spectrin. NMJ size is reduced and the number of synaptic boutons is decreased. Postsynaptic Dlg staining is no longer tightly restricted to regions surrounding the presynaptic boutons. (C) A NMJ lacking postsynaptic β-Spectrin. Postsynaptic Dlg is still enriched around presynaptic boutons, but lacks organization (bottom right). (D) Quantification of presynaptic bouton number on muscles 6 and 7 in segments A2 and A3 as, indicated. Numbers are normalized to wild type in the graph. The loss of postsynaptic α-Spectrin results in a reduction of bouton number to 86 ± 2.5% in segment A2, and to 77 ± 2% in segment A3. The loss of postsynaptic β-Spectrin leads to a reduction in bouton number to 66 ± 2% and 71 ± 2% in segments A2 and A3, respectively. All changes are statistically significant ($P < 0.001$). Bars: (A–C) 10 μm; (magnifications) 5 μm.

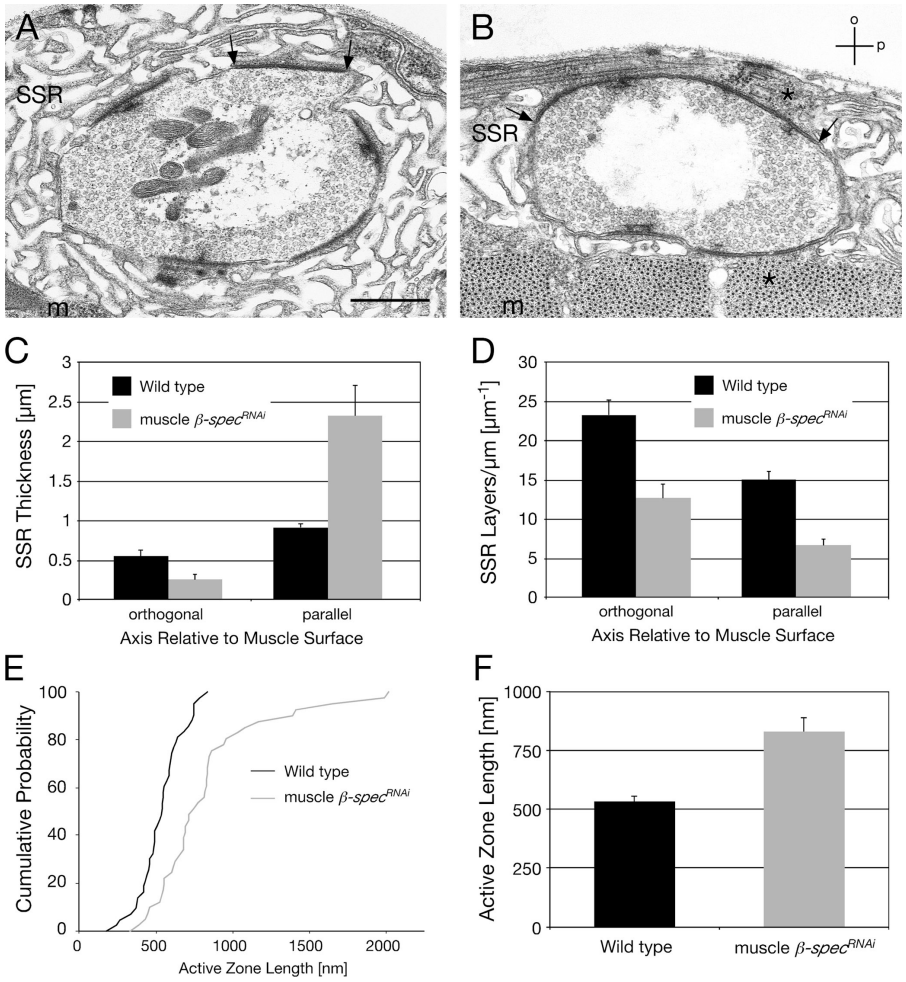

Figure 3. **Ultrastructural analysis of synaptic boutons lacking postsynaptic β-Spectrin.** (A) A cross section of a wild-type synaptic bouton. The postsynaptic muscle membrane folds (SSR) and the muscle fibers (m) are indicated. The presynaptic bouton is completely surrounded by SSR. A representative active zone is demarcated by arrows. (B) A cross section of a synaptic bouton from an animal lacking postsynaptic β-Spectrin. The SSR is severely reduced and almost absent above and below the presynaptic bouton. At many places, including active zones, muscle fibers directly abut the presynaptic membrane (asterisks). The boundaries of a representative active zone are indicated by arrows. (C) Analysis of SSR thickness in wild-type animals and in animals lacking postsynaptic β-Spectrin. (D) Analysis of SSR density in wild type and in animals lacking postsynaptic β-Spectrin. (E) Cumulative probability plot of active zone sizes in wild-type animals and in animals lacking postsynaptic β-Spectrin. (F) Quantification of active zone sizes (wild type = 531 ± 22 nm and *β-spectrin* = 828 ± 59 nm; $P < 0.001$). Error bars represent the SEM. Bars: (A and B) 500 nm.

a PDZ domain containing adaptor protein (PSD-95 homologue) that scaffolds synaptic proteins to the SSR and is required for the elaboration of the SSR during development (Budnik et al., 1996). In wild-type animals, Dlg staining is closely associated with the synaptic bouton (Fig. 2 A). In the absence of postsynaptic α- or β-Spectrin, Dlg remains concentrated at the NMJ; however, it is no longer tightly associated with the presynaptic boutons, occupies a larger domain, and appears disorganized (Fig. 2, B and C). These data suggest that Spectrin is required for the normal development or integrity of the SSR.

We next examined the ultrastructure of the SSR in wild-type and *spectrin*-dsRNA animals. Wild-type boutons are completely surrounded by the SSR membrane network (Fig. 3 A and Fig. S1 A, available at http://www.jcb.org/cgi/content/full/jcb.200607036/DC1). In contrast, synapses lacking postsynaptic β-Spectrin show severe defects in SSR structure (Fig. 3 B; and Fig. S1, B and C). The SSR is generally thinned above and below the synaptic bouton (orthogonal to the muscle surface) and stretched laterally (parallel to the muscle surface; wild-type SSR thickness: orthogonal, 0.545 ± 0.68 µm; parallel, 0.910 ± 0.043 µm; *β-spec* orthogonal: 0.248 ± 0.061 µm; parallel, 2.322 ± 0.391 µm; $n = 10$ boutons each; $P < 0.001$ for both axes compared with wild type; Fig. 3 C). In many cases, muscle tissue directly abuts the presynaptic bouton membrane and active zones (Fig. 3 B, asterisks), a phenotype that is never observed in wild type. In addition, the SSR membranes are generally less compact (wild-type orthogonal, 23.2 ± 1.93 layers/µm; parallel, 15.0 ± 1.1 layers/µm; *β-spec* orthogonal, 12.7 ± 1.9 layers/µm; parallel, 6.7 ± 0.8 layers/µm; $n = 10$ boutons; $P \leq 0.001$ compared with wild type; Fig. 3 D). These ultrastructural data support our light level observations (Fig. 2, B and C), and we conclude that the postsynaptic Spectrin skeleton is required for the normal integrity and development of the SSR.

Postsynaptic Spectrin specifies active zone size and spacing at the NMJ

In addition, our ultrastructural analysis revealed that the size of individual active zones is significantly increased in animals lacking postsynaptic β-Spectrin. Presynaptic active zones were defined as continuous pre- and postsynaptic electron densities that exist at sites with clustered presynaptic vesicles (Fig. 3, A and B; active zones delineated by arrows). Active zone dimension were determined by measuring the length of an uninterrupted electron density. In wild type, active zones have a characteristic length (531 ± 22 nm; $n = 44$) and are spaced at regular intervals throughout the synaptic bouton membrane, which is consistent with previous studies (Atwood et al., 1993;

Meinertzhagen et al., 1998). We find that active zones are significantly larger at NMJs that lack postsynaptic β-Spectrin (mean length, 828 ± 59 nm; $n = 42$; $P < 0.001$; Fig. 3, B–D). In addition, we observe that the spacing between active zones is disturbed, with some active zones forming in very close proximity. These data indicate that postsynaptic Spectrin normally restricts synapse size and controls the regular spacing of synapses at the NMJ.

We next turn to a light level analysis of proteins that localize to the active zone and associated postsynaptic density (Fig. 4). Consistent with our ultrastructural data, we find that Spectrin is required for the specification of normal glutamate receptor cluster size, distribution, and spacing. In wild-type animals, glutamate receptor clusters are of uniform size and evenly distributed within the postsynaptic membrane of the synaptic terminal (Fig. 4, A and A'). If we knock down postsynaptic α- or β-Spectrin, the average size of the glutamate receptor clusters is significantly increased (wt = 0.78 ± 0.01 μm, $n = 536$; *α-spectrin* = 1.08 ± 0.02, $n = 657$; *β-spectrin* = 1.26 ± 0.04, $n = 602$; $P < 0.001$ for all comparisons; Fig. 4, B and B' and C and C'). These data were acquired using an antibody against the GluRII-C subunit of the postsynaptic glutamate receptors. We observed the same phenotype when analyzing the GluRII-A and -B subunits of the glutamate receptors (unpublished data). The change in average cluster size is reflected as a shift of the entire distribution of cluster sizes to larger dimensions (Fig. 4, A'–C'). A similar, significant increase in receptor cluster size was observed in second instar animals (L2; wt = 0.52 ± 0.01, $n = 314$; *β-spectrin* = 0.80 ± 0.03, $n = 320$; $P < 0.001$; Fig. 4, D and E). Together, these data are consistent with the conclusion that the postsynaptic Spectrin skeleton is required to specify the size and organization of the postsynaptic density during synapse development.

We next analyzed the spacing of presynaptic active zones by examining the distribution of the presynaptic protein nc82/Bruchpilot (ELKS/CAST homologue) that marks the center of each presynaptic active zone (Kittel et al., 2006; Wagh et al., 2006). At wild-type synapses, nc82 puncta are evenly spaced throughout the NMJ, and single nc82 puncta are present in opposition to each glutamate receptor cluster (Fig. 5 A; Kittel et al., 2006; Wagh et al., 2006). However, at synapses that lack postsynaptic α- or β-Spectrin, the distribution of nc82 puncta is severely perturbed, and we observe that multiple presynaptic nc82 puncta occur in opposition to single, enlarged glutamate receptor clusters (Fig. 5 B). To quantify this phenotype we determined the ratio between presynaptic nc82 and postsynaptic GluRII-C clusters. At both second and third instar synapses, we find an ~1:1 relationship between nc82 and GluRII-C clusters (second instar: 1.11 ± 0.031, $n = 1{,}788$ nc82 puncta; third instar: 1.4 ± 0.054, $n = 2{,}115$ nc82 puncta). However, at synapses that lack postsynaptic α- or β-Spectrin, this ratio is significantly increased at both second (1.75 ± 0.061, $n = 2{,}201$ nc82 puncta; $P < 0.001$) and third instar NMJs (2.76 ± 0.201, $n = 2{,}210$ nc82 puncta; $P < 0.001$; Fig. 5 C). These data suggest that there is an increase in the number of presynaptic T-bars per postsynaptic density, provided that glutamate receptor clusters imaged at the light level reflect the size of the postsynaptic density. In support of this possibility, the pre- and postsynaptic electron densities that define the active zone and associated postsynaptic density remain precisely aligned in the *β-spectrin*

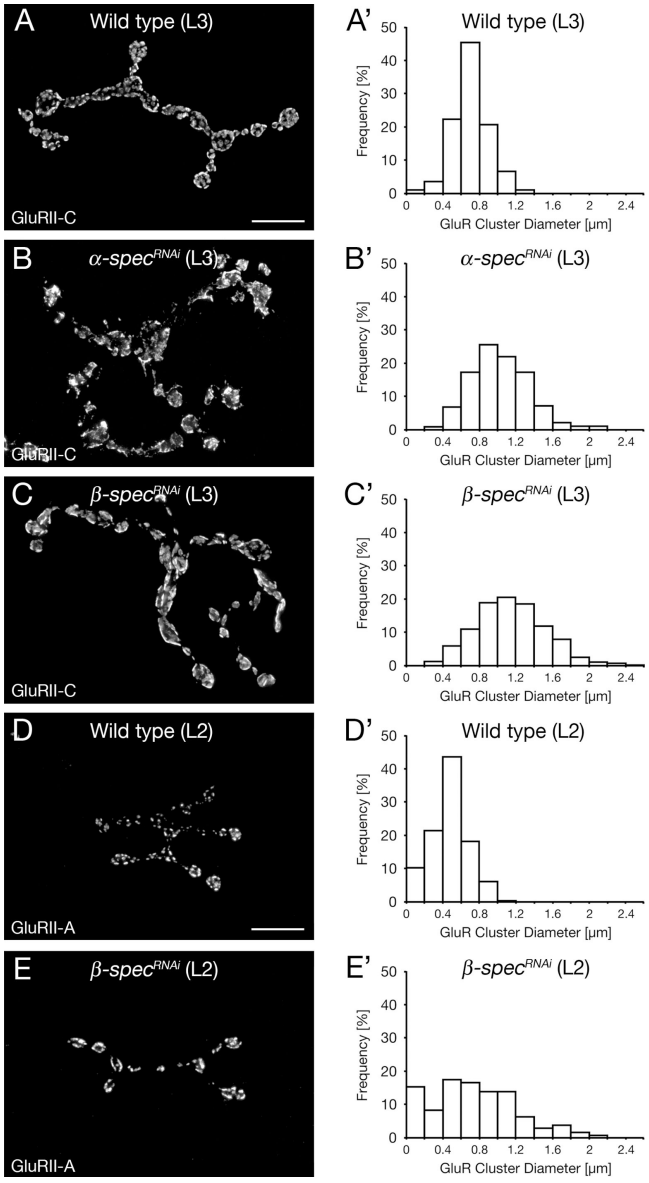

Figure 4. **Analysis of postsynaptic glutamate receptor clusters at synapses lacking postsynaptic α- or β-Spectrin.** (A–C and A'–C') Analysis of postsynaptic glutamate receptor clusters in third instar larvae (L3). (A) A wild-type synapse on muscle 4, stained for the GluRII-C subunit of the postsynaptic glutamate receptor clusters. (A') Frequency distribution of glutamate receptor cluster sizes in wild type. (B) Synapses lacking postsynaptic α-Spectrin show a severe perturbation of glutamate receptor clusters. (B') The frequency distribution reveals a shift toward larger cluster sizes compared with wild type. (C) Synapses lacking postsynaptic β-Spectrin show increased glutamate receptor cluster size and altered organization. (C') The analysis of the frequency distribution reveals a further increase in the number of larger cluster sizes compared with *α-spectrin* and wild type. (D–E') Analysis of postsynaptic glutamate receptor clusters in second instar larvae (L2). (D) A wild-type synapse on muscle 4, stained for the GluRII-A subunit of the postsynaptic glutamate receptor clusters. (D') Frequency distribution of glutamate receptor cluster sizes. (E) A second instar synapse lacking postsynaptic β-Spectrin shows an increase in glutamate receptor cluster size. (E') The frequency distribution reveals a significant increase in cluster size compared with second instar wild-type animals. Bars, (A–E) 10 μm.

RNAi animals, and we observe the presence of multiple T-bars at active zones (Fig. 3 B).

Finally, we determined whether the change in nc82 distribution reflects an increase in the total number of T-bars. We find a slight, though statistically significant, increase in the density of nc82 puncta (wild type: 1.8 ± 0.06 nc82 puncta/area; *β-spectrin*: 2 ± 0.06 n82 puncta/area; $P < 0.05$; Fig. 5 D). Although this increase might contribute to the phenotype, it is more likely that the loss of normal spatial separation is the major cause for the observed phenotype. Thus, our data from both light level and ultrastructural analyses are consistent with the conclusion that the postsynaptic Spectrin skeleton imposes a transsynaptic influence on synapse development to specify synapse size and spacing.

Altered periactive zone organization in the absence of postsynaptic Spectrin

Active zones in both the central and peripheral nervous systems are surrounded by specialized domains, termed the periactive zone, that are enriched with proteins involved in signaling (Coyle et al., 2004), intercellular adhesion, and synaptic vesicle endocytosis (Koh et al., 2004; Marie et al., 2004). We next addressed whether postsynaptic Spectrin is necessary to define and organize the active zone versus periactive zone domains.

We first analyzed two reporters that define the periactive zone within the postsynaptic membrane, Shaker-GFP and the cell adhesion molecule Fasciclin II (Fas II). These markers are organized into a postsynaptic periactive zone network that surrounds glutamate receptor clusters (Fig. 6, A and C). Both Sh-GFP and Fas II depend on Dlg for synaptic localization (Thomas et al., 1997; Zito et al., 1997). However, Sh-GFP is only present in the postsynaptic membrane, whereas Fas II is present pre- and postsynaptically and functions as a homophilic cell adhesion molecule. At synapses that lack postsynaptic α- or β-Spectrin, both Sh-GFP and Fas II are severely disorganized, but remain separate from clusters of postsynaptic glutamate receptors (Fig. 6 B and not depicted; wild type percentage of colocalization Sh-GFP with GluR-IIC: 17.6 ± 1.5%; *α-spec*: 5.6 ± 0.9%; $n = 9$; $P < 0.001$). In addition, in the absence of postsynaptic α- or β-Spectrin, Fas II staining still circumscribes p21-activated kinase (Pak) staining, a postsynaptic density marker that colocalizes with glutamate receptors (Fig. 6 D; Albin and Davis, 2004; wild type percentage of colocalization Fas II with Pak: 14.7 ± 1.0%; *β-spec*: 9.8 ± 0.7%; $n = 11$; $P < 0.001$). Thus, postsynaptic periactive zone membrane markers, although altered in appearance, remain in a discrete membrane domain that is juxtaposed to the postsynaptic density.

Next, we examined the organization of the presynaptic, cytoplasmic protein Nervous Wreck (Nwk) that localizes to the periactive zone domain (Coyle et al., 2004). At wild-type synapses, Nwk and Fas II partially colocalize and surround the presynaptic active zone defined by nc82 (Fig. 6 E and not depicted; Coyle et al., 2004; Marie et al., 2004). In the absence of postsynaptic α- or β-Spectrin, the distribution of presynaptic Nwk and Fas II is altered; however, the amount of colocalization between Nwk and Fas II remains unchanged (wild type percentage of colocalization Nwk with Fas II: 37.1 ± 2.2%; *β-spec*: 36.0 ± 1.5%; Fig. 6 F). A similar effect can be observed for the distribution of the presynaptic periactive zone protein Dap160/intersectin (unpublished data). Again, the presynaptic periactive zone domain defined by Nwk, Fas II, and Dap160, although disorganized in the absence of postsynaptic Spectrin, does not

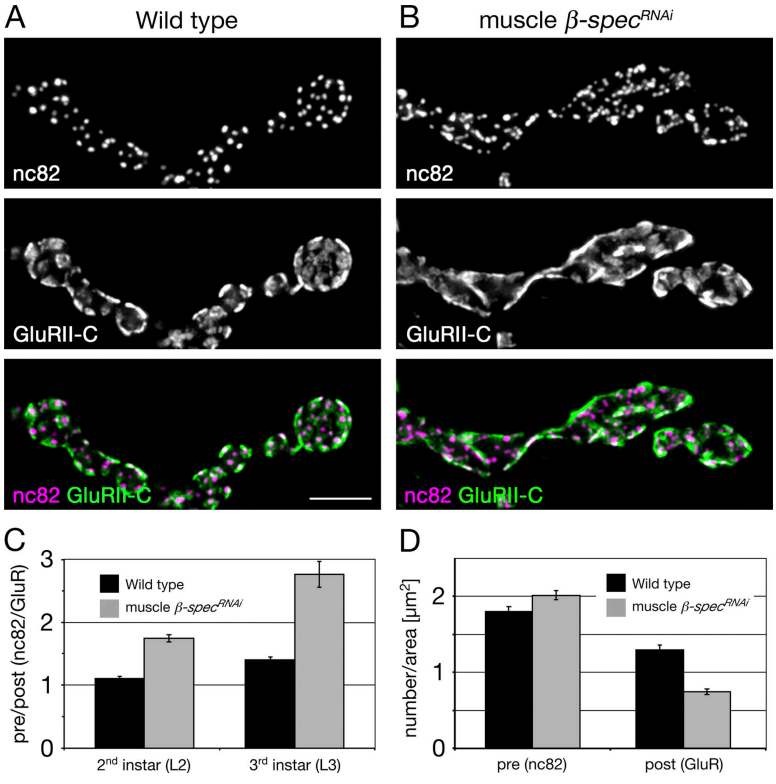

Figure 5. **Postsynaptic Spectrin organizes pre- and postsynaptic synapse markers.** (A) A wild-type synapse on muscle 4, stained for the presynaptic active zone marker nc82 and the postsynaptic glutamate receptor cluster subunit GluRII-C. (B) A synapse on muscle 4 lacking postsynaptic β-Spectrin. Multiple puncta of the presynaptic active zone marker nc82 accumulate opposite single, enlarged postsynaptic GluRII-C receptor clusters. (C) Quantification of presynaptic nc82 and postsynaptic GluRII-C puncta reveals a significant increase in the ratio of presynaptic nc82 puncta per postsynaptic glutamate receptor cluster in both L2 and L3 larvae in the absence of postsynaptic β-Spectrin, compared with wild type. (D) Quantification of presynaptic nc82 puncta and postsynaptic glutamate receptor clusters per NMJ area. Error bars represent the SEM. Bars, (A and B) 10 μm.

invade the active zone domain defined by nc82. Collectively, these data support the conclusion that postsynaptic Spectrin defines active zone dimensions, but does not specify the identities of active zone or periactive zone domains.

Altered synaptic function in the absence of postsynaptic α- or β-Spectrin

To assess the functional consequences of altered synapse size and spacing, we recorded from NMJs lacking postsynaptic α- or β-Spectrin. Compared with wild-type synapses, we observe a dramatic increase in the average amplitude of spontaneous miniature release events (mepsp [miniature excitatory postsynaptic potential {EPSP}]; quantal size) after the loss of either α- or β-Spectrin (Fig. 7, A and B). There was no statistically significant change in muscle input resistance (wild type: 7 ± 0.6 MΩ; *α-spec*, 7 ± 0.3 MΩ; *β-spec*, 9 ± 1.0 MΩ; $n = 11$; $P = 0.06$ for *β-spec* compared with wild type) or in the average membrane resting potential (wild type: −73 ± 2.1 mV; *α-spec*, −71.2 ± 1.2 mV; *β-spec*, 74.5 ± 4.1 mV; $n = 11$; $P > 0.1$ for both genotypes compared with wild type). The increase in quantal size could be caused by an increase in presynaptic vesicle size, an increase in the concentration of vesicular glutamate, a change in the spacing of pre- and postsynaptic membranes, or an increase in postsynaptic glutamate receptor sensitivity. An ultrastructural analysis of neurotransmitter vesicle sizes at active zones revealed no significant difference between animals lacking postsynaptic β-Spectrin and wild-type animals (Fig. 7 C; $P > 0.01$). In addition, pre- and postsynaptic electron densities remain perfectly aligned and we did not find any evidence of altered active zone integrity. Therefore, we hypothesize that the observed changes in mepsp amplitudes are related to the observed differences in glutamate receptor organization. One possibility is that there has been a change in the sensitivity or density of postsynaptic glutamate receptors; however, we cannot exclude other possibilities at this time.

We next assayed presynaptic neurotransmitter release by recording EPSP amplitudes in response to single action potentials in the motoneuron. In animals lacking postsynaptic

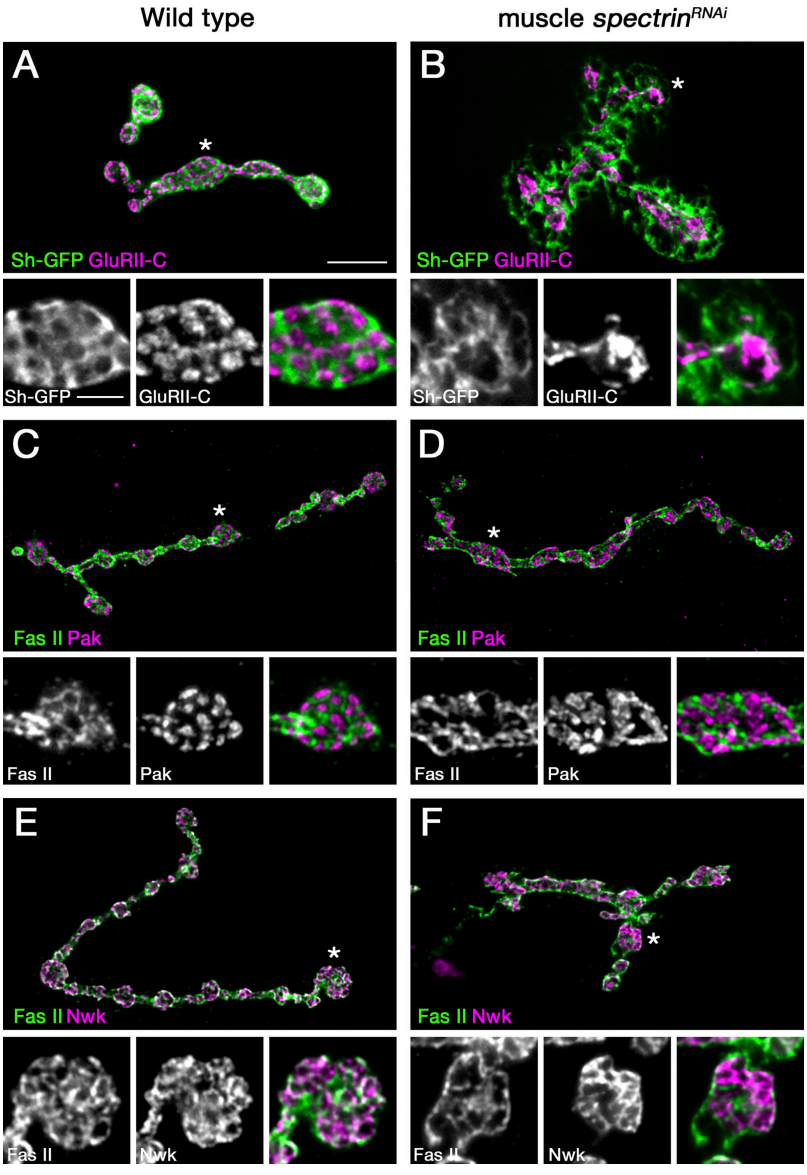

Figure 6. **Postsynaptic Spectrin is required for the organization of active zone and periactive zone components.** All images are of NMJs at muscle 4. Smaller images show higher magnifications and single channels from the areas indicated by the asterisks. (A) A wild-type synapse stained for the postsynaptic density marker GluRII-C and the postsynaptic periactive zone reporter Sh-GFP. Sh-GFP staining circumscribes the evenly distributed GluRII-C receptor clusters. (B) At a synapse lacking postsynaptic α-Spectrin, Sh-GFP is no longer confined to the area directly surrounding the postsynaptic receptor clusters and loses its latticelike appearance. (C) A wild-type synapse stained for the postsynaptic active zone marker Pak and the transsynaptic cell adhesion molecule Fas II, which localizes to the periactive zone. Fas II forms a honeycomb-like network that precisely surrounds Pak staining. (D) At synapses lacking postsynaptic β-Spectrin, Pak clusters become bigger and less regular shaped. The Fas II network is less regular, but still surrounds Pak-positive clusters. (E) A wild-type synapse stained for Fas II and the cytoplasmic presynaptic periactive zone marker Nwk. Fas II and Nwk partially colocalize and surround the presynaptic active zone. (F) At synapses lacking postsynaptic β-Spectrin, Fas II and Nwk lose their regular organization. Bars: (A–F) 10 μm; (magnifications) 3 μm.

α-Spectrin, we observe an increase in EPSP amplitude that parallels the increase in quantal size (Fig. 7 A). However, after the loss of β-Spectrin, EPSP amplitudes are only slightly increased, despite the large increase in quantal size. As a result, we calculate a significant decrease in presynaptic neurotransmitter release (quantal content; Fig. 7 A). We hypothesize that the deficit in presynaptic release may be secondary to the more severe decrease in bouton numbers observed in animals lacking postsynaptic β-Spectrin compared with α-Spectrin (Fig. 2 D). Alternatively, it could indicate additional functions of β-Spectrin that are α-Spectrin independent.

Spectrin recruits Ankyrin to the postsynaptic membrane during synapse development

Studies examining a variety of tissue types in organisms ranging from *D. melanogaster* to vertebrate species demonstrate that the Spectrin skeleton is recruited to the plasma membrane through interactions with the adaptor protein Ankyrin (Dubreuil et al., 1996; Jefford and Dubreuil, 2000; Bennett and Baines, 2001; Ango et al., 2004). The *D. melanogaster* genome encodes two different Ankyrin genes, *ankyrin* (*ank*) and *ankyrin 2* (*ank2*; Dubreuil and Yu, 1994; Bouley et al., 2000). It has been demonstrated that Ank2 expression is restricted to the nervous system (Bouley et al., 2000; Hortsch et al., 2002). Therefore, we focused our analysis on Ank, which is present at the larval NMJ and colocalizes with α-Spectrin (Fig. S2, A–C, available at http://www.jcb.org/cgi/content/full/jcb.200607036/DC1) and Dlg (Fig. 8, A–C). The *ank* gene is encoded on the genetically intractable fourth chromosome of *D. melanogaster*, and no mutations in *ank* have been identified so far. The expression of *ank* dsRNA using the muscle-specific driver line BG57-Gal4 enables us to knock down Ank protein in the muscle of third instar larvae (Fig. 8, D–F). In animals lacking postsynaptic Ank, we do not observe a significant change in α- or β-Spectrin distribution in the SSR that surrounds the presynaptic terminal (Fig. S1, E and F). Thus, in contrast to other systems, Ank is not required for the recruitment of Spectrin to postsynaptic muscle membranes at the NMJ. In contrast, the knockdown of β-Spectrin leads to a near complete loss of Ank from the SSR (Fig. 8 G). This indicates that β-Spectrin is necessary to localize Ank to the NMJ. In addition, we find that the loss of postsynaptic α-Spectrin results in a disorganization of Ank within the SSR suggesting that Ank remains bound to β-Spectrin that persists in the SSR in the absence of postsynaptic α-Spectrin (Fig. 1 F).

The disruption of Ank localization could potentially contribute to the phenotypes observed in animals lacking postsynaptic α- or β-Spectrin. Although the structure and integrity of the postsynaptic SSR is not affected in animals lacking postsynaptic Ank (Fig. 8 E), we observe a slight, statistically significant increase in the average size of glutamate receptor clusters

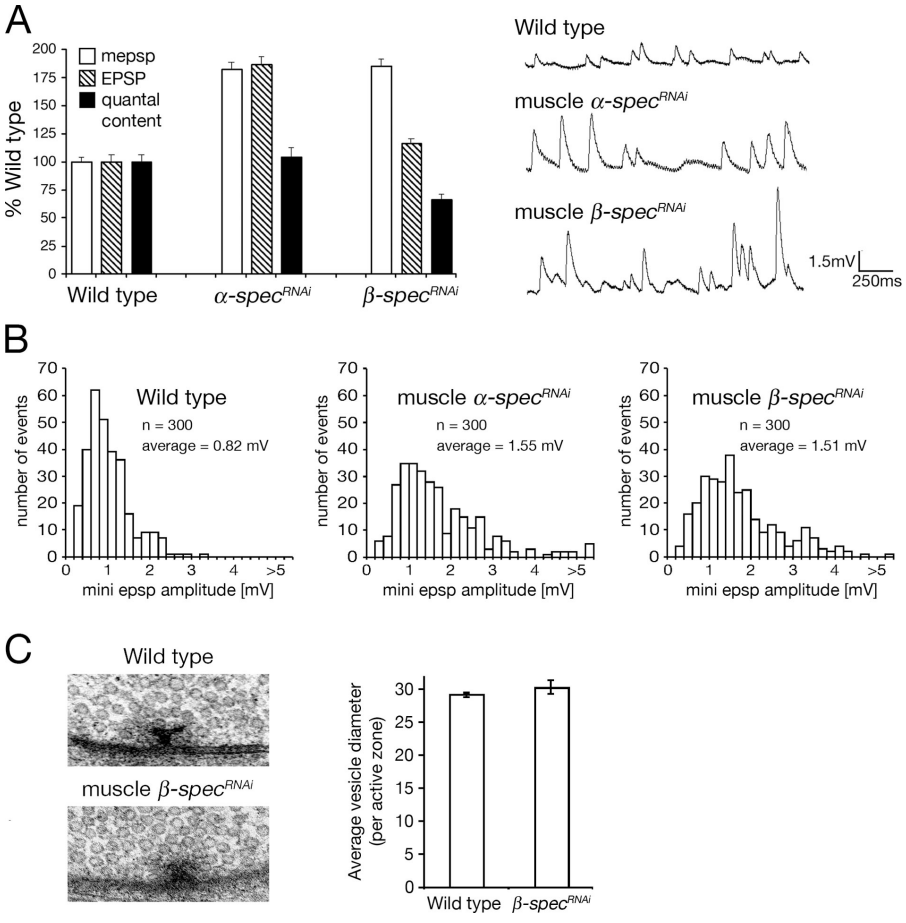

Figure 7. **Synapses lacking postsynaptic α- or β-Spectrin show an increase in quantal size.** (A) Quantification of the average mepsp amplitude (quantal size), EPSP amplitude, and quantal content in wild type and in animals lacking postsynaptic α- or β-Spectrin. Measurements are normalized to wild type to allow display of the data on a single graph. At synapses lacking postsynaptic α- or β-Spectrin there is a significant increase in quantal size compared with wild type (82% increase for *α-spectrin* and 85% increase for *β-spectrin*; $P < 0.001$). At synapses lacking postsynaptic α-Spectrin, EPSP amplitudes are larger than wild type, and there is no change in quantal content compared with wild type. At synapses lacking postsynaptic β-Spectrin, EPSPs are larger than wild type, but there is a significant decrease in quantal content. Representative mepsp traces are shown. (B) Histograms of mepsp amplitude distributions in wild type and in animals lacking postsynaptic α- or β-Spectrin. (C) Ultrastructural analysis of average synaptic vesicle diameters for wild-type synapses and synapses lacking postsynaptic β-Spectrin. There is no change in the average vesicle diameter at synapses lacking postsynaptic β-Spectrin compared with wild type. Representative images of active zones are shown at left. Error bars represent the SEM.

(wild type 0.8 ± 0.01μm, $n = 515$; *ankyrin* 0.96 ± 0.03 μm, $n = 410$; $P < 0.001$; Fig. S3, B and C, available at http://www.jcb.org/cgi/content/full/jcb.200607036/DC1). Consistently, we find a small, but statistically significant, increase in quantal size in animals lacking postsynaptic Ank compared with wild-type controls (wt = 0.93 ± 0.06 mV; *ank* = 1.28 ± 0.10 mV; $P < 0.05$). In conclusion, β-Spectrin is required for the efficient localization of Ank to the postsynaptic SSR, and Ank contributes to the Spectrin-dependent control of synapse development.

Discussion

We demonstrate that the postsynaptic Spectrin skeleton is necessary for the normal size and spacing of synapses at the NMJ, with both pre- and postsynaptic compartments of the synapse being altered in parallel. Although synapse size and positioning are changed, we still observe a perfect alignment of the presynaptic active zone and the postsynaptic density and segregation between active zone and periactive zone components on both sides of the synapse. Mechanistically, β-Spectrin is required for the localization of α-Spectrin and Ankyrin to the postsynaptic membrane. These data suggest that the postsynaptic Spectrin skeleton imposes a transsynaptic organization that is necessary for the normal development of both the presynaptic active zone and the opposing postsynaptic density.

How does the postsynaptic Spectrin skeleton restrict synapse size and spacing?

α- and β-Spectrin heterotetramers have a length of ∼180–265 nm when purified from membrane preparations of *D. melanogaster* or from preparations of vertebrate erythrocytes or brain tissue (Shotton et al., 1979; Bennett et al., 1982; Dubreuil et al., 1987). These heterotetramers can bind to short actin fragments and form a stereotypic hexagonal lattice that is linked to the plasma membrane (Byers and Branton, 1985; Liu et al., 1987). Interestingly, the dimension of one of these hexagonal Spectrin–actin structures closely corresponds to the size of an average active zone at the *D. melanogaster* NMJ. The diameter of an average active zone is ∼500–600 nm (Fig. 3 D) (Atwood et al., 1993; Meinertzhagen et al., 1998), which corresponds to the size of two Spectrin heterotetramers linked by actin filaments (Fig. 9, B and C). Therefore, the organization of a postsynaptic Spectrin–actin network into a hexagonal lattice could provide a framework upon which synapse development is organized (Fig. 9, B and C).

Restriction of glutamate receptors to the postsynaptic density

There are several possible scenarios for how a Spectrin–actin lattice could restrict synapse size. In one model, the Spectrin–actin network could stabilize glutamate receptors through direct or indirect interactions, as previously hypothesized (Bloch and Morrow, 1989; Wechsler and Teichberg, 1998; Shen et al., 2000). In a second model, the lateral expansion of active zones might be constrained by the dimension of the postsynaptic, hexagonal Spectrin–actin lattice (Fig. 9). This lattice could be used to organize the scaffolding protein Dlg, which, in turn, could confine the distribution of integral periactive zone proteins to limit the dimensions of the postsynaptic density (Fig. 9 C). In support of this model, ultrastructural reconstructions revealed a significant increase in the size of active zones at the NMJ of *dlg* mutants (Karunanithi et al., 2002). Finally, the changes in glutamate receptor cluster size and spacing could be a secondary consequence of the disruption of the postsynaptic membrane network that composes the SSR. However, other mutations that affect SSR density and organization do not cause an increase in active zone size (Parnas et al., 2001; Packard et al., 2002).

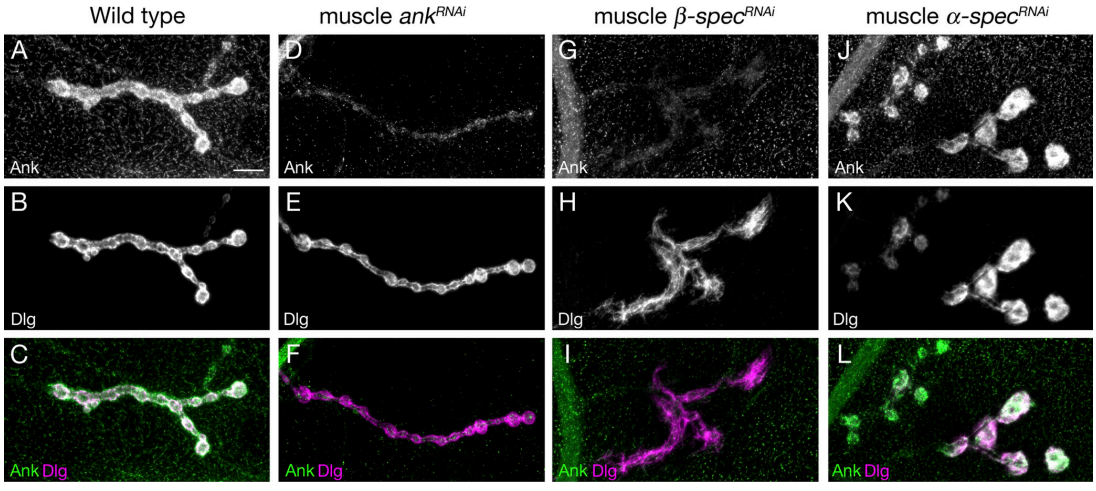

Figure 8. **Postsynaptic α- and β-Spectrin are required for the normal localization of postsynaptic Ankyrin.** (A–C) A wild-type synapse on muscle 4 stained for Ank and Dlg. Ank is present in the T-tubules throughout the muscles and highly enriched in the SSR of 1b and 1s boutons. (D–F) The postsynaptic expression of *ank* dsRNA results in the elimination of Ank in the muscle. Ank can no longer be detected in the T-tubules or the SSR. Presynaptic Ank becomes evident in the absence of postsynaptic Ank. Dlg organization within the postsynaptic SSR remains unaltered in the absence of postsynaptic Ank. (G–I) A muscle 4 synapse that lacks postsynaptic β-Spectrin. The SSR is clearly disturbed and Dlg organization is disrupted. Ank is almost completely absent from the SSR, but is still present in the T-tubule network (G). (J–L) A muscle 4 synapse that lacks postsynaptic α-Spectrin. The organization of the SSR is severely disturbed but Ank is still present at the SSR and colocalizes with Dlg. Bar, (A–L) 10 μm.

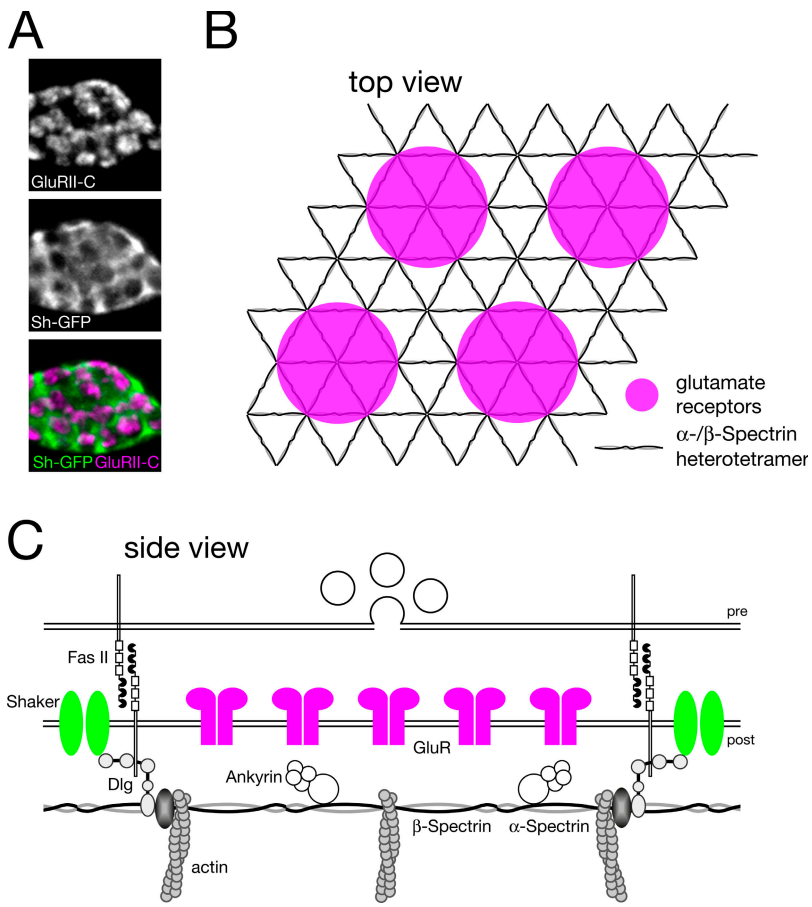

Figure 9. **A postsynaptic Spectrin–actin network can define synapse dimensions and spacing.** (A) Staining of GluRII-C receptors and Sh-GFP (Fig. 6). (B) Top view of a proposed α-/β-Spectrin hexagonal network. In this model, a unit of six Spectrin heterotetramers linked by actin filaments could participate in the organization of synapse size and spacing. (C) Side view of a single synapse. Spectrin heterotetramers are linked through interactions of β-Spectrin with short actin filaments. The postsynaptic Spectrin–actin network could participate in the localization of periactive zone proteins such as Dlg to the borders of the active zone. Dlg, in turn, could then bind and scaffold additional periactive zone proteins, including Fas II and Shaker.

The postsynaptic Spectrin skeleton organizes SSR formation

In the absence of postsynaptic α- or β-Spectrin, the postsynaptic membrane folds (SSR) no longer tightly surround the presynaptic bouton, but are spread laterally and are severely thinned above and below the synaptic bouton. There are two possible explanations for this phenotype. One possibility is that disorganized Dlg directs the inappropriate formation of SSR. Previous studies have demonstrated that Dlg is necessary and sufficient for SSR formation in *D. melanogaster* (Budnik et al., 1996), and the analysis of *α-* and *β-spectrin*–null mutant embryos suggest that Spectrin is required for the localization of Dlg to the synapse (Featherstone et al., 2001). Alternatively, the SSR organization could be disrupted in response to muscle contractions in the absence of postsynaptic α- or β-Spectrin. The Spectrin skeleton could serve as a protective network because of its elastic properties (Bennett and Baines, 2001). The loss of mechanoprotection might explain the lateral stretch of SSR and the reduction of SSR orthogonal to the muscle surface.

Establishment of a Spectrin-actin network at the postsynaptic membrane

Our analysis reveals interesting insights into the assembly of the Spectrin skeleton at the postsynaptic membrane. We demonstrate that β-Spectrin is required for the localization of α-Spectrin and Ank to the postsynaptic plasma membrane, whereas α-Spectrin is only required for the appropriate localization of β-Spectrin and Ank within the SSR. Interestingly, the knock down of postsynaptic Ank does not significantly influence the localization of α- or β-Spectrin (Fig. 8). This differs from previous observations in other *D. melanogaster* tissues and in vertebrates where Ank is required for the localization of β-Spectrin to specific membrane domains and Spectrin then stabilizes these complexes (Dubreuil et al., 1996, 2000; Jenkins and Bennett, 2001; Komada and Soriano, 2002; Mohler et al., 2004). Thus, either the membrane localization of β-Spectrin depends on interactions with other adaptor or transmembrane molecules or β-Spectrin binds directly to phospholipid components of the postsynaptic membrane through its membrane association domains (Bennett and Baines, 2001).

Spectrin function during development, plasticity, and disease in the vertebrate nervous system

It is interesting to speculate that Spectrin may function to determine active zone dimensions in the vertebrate nervous system. At central synapses, active zone dimensions and spacing are precisely controlled, implying molecular regulation (Schikorski and Stevens, 1997, 1999; Satzler et al., 2002). The importance of controlling active zone dimensions is underscored by a correlation between presynaptic release probability and active zone dimension at hippocampal synapses (Schikorski and Stevens, 1997). A remaining question is whether the Spectrin skeleton could be involved in the activity-dependent regulation of active

zone size and efficacy (Shen et al., 2000; Bennett and Baines, 2001). It is interesting to note that the increase in active zone size at the *D. melanogaster* NMJ after the knock down of postsynaptic Spectrin does not lead to an apparent increase in release probability. However, given the developmental time frame of these manipulations, it is possible that homeostatic mechanisms readjust presynaptic release to baseline levels.

The importance of the Spectrin skeleton in the vertebrate nervous system has been underscored by the recent discovery that mutations in human *β-III spectrin* cause spinocerebellar ataxia type 5 (Ikeda et al., 2006). Spinocerebellar ataxia type 5 results in Purkinje cell loss, cerebellar cortical atrophy, and neuromuscular defects (Ikeda et al., 2006). Importantly, one of the human mutations in *β-III spectrin* is a point-mutation within the actin-binding domain that is essential for the formation of an intact Spectrin–actin network (Ikeda et al., 2006). As the human mutations are dominant, it indicates that even small changes in the robustness of the Spectrin–actin network might result in severe neurological defects and disease.

Materials and methods

Fly stocks

Flies were maintained at 25°C on normal food. The following strains were used in this study: w^{1118} (wild type), *BG57*-GAL4 (muscle expression from mid–first-instar on; Budnik et al., 1996), *da*-GAL4 (ubiquitous expression; Wodarz et al., 1995), *MHC-Shaker*-GFP (Zito et al., 1997), UAS-*α-spectrin*-dsRNA, and UAS-*β-spectrin*-dsRNA (Pielage et al., 2005). We recapitulated the expression pattern of BG57-Gal4 using a UAS-mCD8-GFP transgene (Lee and Luo, 1999). We observed strong expression in postembryonic muscle and some expression in peripheral neurons that send projection axons into the CNS, as previously reported (Budnik et al., 1996). We did not observe any expression in motoneuron axons. To ensure that there is no expression in the motoneurons projecting to muscles 6/7 that might not be detectable at the light level, we expressed UAS–tetanus toxin (Sweeney et al., 1995) using BG57-Gal4. The expression of UAS–tetanus toxin in neurons abolishes evoked neurotransmission (Broadie et al., 1995; Sweeney et al., 1995). We did not observe any significant decrease in the amplitude of EPSPs at muscles 6/7 in these animals, demonstrating the tissue-specificity of the BG57-Gal4 driver line.

Generation of the UAS–*ankyrin*–dsRNA construct and germline transformation

We used the pWIZ-Vector (R. Carthew, Northwestern University, Evanston, IL; Lee and Carthew, 2003) to generate the UAS-*ankyrin*-dsRNA construct. The target sequence was selected to avoid significant homology with any other *D. melanogaster* gene to ensure specificity of the resulting dsRNA. We introduced XbaI restriction sites (underlined) to allow direct cloning into the pWIZ vector (Lee and Carthew, 2003). The following primers were used to amplify a 593-bp fragment of the *ankyrin* open reading frame starting at position 3,835 of the *ankyrin-RA* cDNA: 5′GGGCGGGTTCTAGAAAAACGAATTTCCCAAACGGAAGC-3′ and 5′-GGGCGGGTTCTAGAAAAGGCCAGTCACTTCCTAAGTGGC-3′. The DNA fragment was amplified from wild-type genomic DNA and cloned into pWIZ following the methods used by Lee and Carthew (2003). The construct was confirmed by sequencing. Transgenic flies were generated by standard methods. At least two independent transgene insertions were established for chromosomes 2 and 3.

Immunocytochemistry

Wandering third instar larvae were dissected in HL3 saline and fixed either with 4% paraformaldehyde/PBS for 15 min or in Bouin's fixative (Sigma-Aldrich) for 2 min. Primary antibodies were applied at 4°C overnight. Primary antibodies were used at the following dilutions: anti-Bruchpilot (nc82) 1:100 (gift from E. Buchner, Theodor-Boveri-Institut für Biowissenschaften, Würzburg, Germany); anti–α-Spectrin (3A9) 1:50; anti–D-GluRIIA (8B4D2) 1:10; anti–Fasciclin II (1D4) 1:10 (all provided by the Developmental Studies Hybridoma Bank, Iowa); rabbit anti–D-GluRIIB (1:2,500), rabbit anti–D-GluRIIC (1:5,000; both antibodies were gifts from A. DiAntonio, Washington University, St. Louis, MO); rabbit anti-Dlg 1:5,000 (gift from V. Budnik, University of Massachusetts, Worcester, MA); rabbit anti–α-Spectrin 1:500, rabbit anti–β-Spectrin 1:500, rabbit anti-Ankyrin 1:500 (all gifts from R. Dubreuil, University of Illinois, Chicago, IL); rabbit anti-Pak 1:500 (gift from L. Zipursky, University of California, Los Angeles, CA); rabbit anti-synaptotagmin 1:500; rabbit anti-Dap160 1:200; rat anti–Nervous wreck 1:1,000 (gift from B. Ganetzky, University of Wisconsin, Madison, WI). All secondary antibodies and Cy3- and Cy5-conjugated anti-HRP were obtained from Jackson ImmunoResearch Laboratories and Invitrogen and used at a 1:200–1:1,000 dilution and applied for 1–2 h at RT. Larval preparations were mounted in Vectashield (Vector Laboratories). Images were captured at RT using an inverted microscope (Axiovert 200; Carl Zeiss MicroImaging, Inc.), a 100×/1.4 NA Plan Apochromat objective (Carl Zeiss MicroImaging, Inc.), and a cooled charge-coupled device camera (CoolSNAP HQ; Roper Scientific). Intelligent Imaging Innovations (3i) software was used to capture, process, and analyze images. Glutamate receptor cluster size and number were analyzed in the original 3D images to ensure precise measurements and distinction between neighboring clusters. The percentage of colocalization between different synaptic proteins was analyzed in single median focal planes using automated routines in the 3i software.

Western Blots

For each genotype, 10 larval body-wall muscle preparations were homogenized in 2% SDS buffer (50 mM Tris-HCl, pH 6.8, 25 mM KCl, 2 mM EDTA, 0.3 M sucrose, and 2% SDS) on ice. After centrifugation at 5,000 *g*, samples were boiled for 5 min in sample buffer (includes DTT and β-mercaptoethanol) and proteins were separated in a 7.5% SDS-PAGE gel and immunoblotted with primary antibodies overnight at 4°C. Protein bands were visualized with HRP-conjugated secondary antibodies and enhanced chemiluminescence reagents (GE Healthcare).

Electrophysiology

Third instar larvae were selected and dissected according to previously published techniques (Pielage et al., 2005). Whole-muscle recordings were performed on muscle 6 in abdominal segment A3 using sharp microelectrodes (12–16 MΩ). Recordings were selected for analysis only if resting membrane potentials were more hyperpolarized than –60 mV and if input resistances were greater than 5 MΩ. The mean spontaneous mepsp amplitude was quantified by measuring the amplitude of ~100–200 individual spontaneous release events per synapse. The mean per-synapse mepsp amplitudes were then averaged for each genotype. Measurement of mepsp amplitudes was semi-automated (Synaptosoft). The mean super-threshold–evoked EPSP amplitude was calculated for each synapse, ensuring that both motor axons innervating muscle 6 in segment A3 were recruited. Quantal content was calculated as the mean EPSP amplitude divided by the mean mepsp amplitude. Quantal content was determined for each synapse and averaged across synapses to generate the mean quantal content for each genotype. Data for steady-state synaptic transmission were acquired in HL3 saline (0.3 mM Ca^{2+} and 10 mM Mg^{2+}). Data were collected using an amplifier (Axoclamp 2B; Axon Instruments), analogue-to-digital board (Digidata 1200B; Axon Instruments), a Master-8 stimulator (AMPI,) and PClamp software (Axon Instruments). Data were analyzed offline using Mini-Analysis software (Synaptosoft, Inc.).

Electron microscopy

Third instar larvae were prepared for electron microscopy as previously described (Pielage et al., 2005). For the analysis of active zone length, SSR phenotypes, and vesicle diameters, the largest diameter section of 1b boutons corresponding to the bouton midline were selected. To determine SSR thickness, the distance between the presynaptic membrane and the distalmost SSR membrane was measured. Four different measurements at 90° angles from each other, starting orthogonal to the muscle surface, were performed for each bouton. The two orthogonal and the two parallel measurements were averaged and analyzed as separate datasets. To analyze the density of the SSR, we counted the number of membrane segments crossed by the line used to measure the SSR thickness. Four measurements at 90° angles were performed and averaged as above. This number was divided by the SSR thickness to calculate the number of layers per μm. Average synaptic vesicle diameters were measured for vesicles within 250 nm of the active zone. The average vesicle diameter was determined for each active zone, and then measurements per active zone were averaged for each genotype.

Online supplemental material

Fig. S1 shows low magnification images of the ultrastructural analysis of synaptic boutons in wild type and in animals lacking postsynaptic β-Spectrin. Fig. S2 shows that postsynaptic Ankyrin is not required for the localization of α- or β-Spectrin to the postsynaptic membrane (SSR). Fig. S3 shows that postsynaptic Ankyrin is required for the control of glutamate receptor cluster size. Online supplemental material is available at http://www.jcb.org/cgi/content/full/jcb.200607036/DC1.

We would like to thank A. DiAntonio, E. Buchner, V. Budnik, R. Dubreuil, B. Ganetzky, L. Zipursky and the Developmental Studies Hybridoma Bank, Iowa for antibodies and R. Carthew for the pWIZ vector. We thank members of the Davis laboratory including Heather Heerssen, Benjamin Eaton and Catherine Massaro for critical reading of prior versions of this manuscript and Dion Dickman for experimental assistance.

This work was supported by a fellowship of the Deutsche Forschungsgemeinschaft to J. Pielage and National Institutes of Health grant NS047342 to G.W. Davis.

Submitted: 10 July 2006
Accepted: 6 October 2006

References

Albin, S.D., and G.W. Davis. 2004. Coordinating structural and functional synapse development: postsynaptic p21-activated kinase independently specifies glutamate receptor abundance and postsynaptic morphology. *J. Neurosci*. 24:6871–6879.

Ango, F., G. di Cristo, H. Higashiyama, V. Bennett, P. Wu, and Z.J. Huang. 2004. Ankyrin-based subcellular gradient of neurofascin, an immunoglobulin family protein, directs GABAergic innervation at Purkinje axon initial segment. *Cell*. 119:257–272.

Atwood, H.L., C.K. Govind, and C.F. Wu. 1993. Differential ultrastructure of synaptic terminals on ventral longitudinal abdominal muscles in *Drosophila* larvae. *J. Neurobiol.* 24:1008–1024.

Bennett, V., and A.J. Baines. 2001. Spectrin and ankyrin-based pathways: metazoan inventions for integrating cells into tissues. *Physiol. Rev.* 81:1353–1392.

Bennett, V., J. Davis, and W.E. Fowler. 1982. Brain spectrin, a membrane-associated protein related in structure and function to erythrocyte spectrin. *Nature*. 299:126–131.

Bloch, R.J., and J.S. Morrow. 1989. An unusual beta-spectrin associated with clustered acetylcholine receptors. *J. Cell Biol.* 108:481–493.

Bouley, M., M.Z. Tian, K. Paisley, Y.C. Shen, J.D. Malhotra, and M. Hortsch. 2000. The L1-type cell adhesion molecule neuroglian influences the stability of neural ankyrin in the *Drosophila* embryo but not its axonal localization. *J. Neurosci.* 20:4515–4523.

Bredt, D.S., and R.A. Nicoll. 2003. AMPA receptor trafficking at excitatory synapses. *Neuron*. 40:361–379.

Broadie, K., A. Prokop, H.J. Bellen, C.J. O'Kane, K.L. Schulze, and S.T. Sweeney. 1995. Syntaxin and synaptobrevin function downstream of vesicle docking in *Drosophila*. *Neuron*. 15:663–673.

Budnik, V., Y.H. Koh, B. Guan, B. Hartmann, C. Hough, D. Woods, and M. Gorczyca. 1996. Regulation of synapse structure and function by the *Drosophila* tumor suppressor gene dlg. *Neuron*. 17:627–640.

Byers, T.J., and D. Branton. 1985. Visualization of the protein associations in the erythrocyte membrane skeleton. *Proc. Natl. Acad. Sci. USA*. 82:6153–6157.

Coyle, I.P., Y.H. Koh, W.C. Lee, J. Slind, T. Fergestad, J.T. Littleton, and B. Ganetzky. 2004. Nervous wreck, an SH3 adaptor protein that interacts with Wsp, regulates synaptic growth in *Drosophila*. *Neuron*. 41:521–534.

Dubreuil, R.R., and J. Yu. 1994. Ankyrin and beta-spectrin accumulate independently of alpha-spectrin in *Drosophila*. *Proc. Natl. Acad. Sci. USA*. 91:10285–10289.

Dubreuil, R., T.J. Byers, D. Branton, L.S. Goldstein, and D.P. Kiehart. 1987. *Drosophilia* spectrin. I. Characterization of the purified protein. *J. Cell Biol.* 105:2095–2102.

Dubreuil, R.R., G. MacVicar, S. Dissanayake, C. Liu, D. Homer, and M. Hortsch. 1996. Neuroglian-mediated cell adhesion induces assembly of the membrane skeleton at cell contact sites. *J. Cell Biol.* 133:647–655.

Dubreuil, R.R., P. Wang, S. Dahl, J. Lee, and L.S. Goldstein. 2000. *Drosophila* β spectrin functions independently of α spectrin to polarize the Na,K ATPase in epithelial cells. *J. Cell Biol.* 149:647–656.

Eaton, B.A., and G.W. Davis. 2005. LIM Kinase1 controls synaptic stability downstream of the type II BMP receptor. *Neuron*. 47:695–708.

Eaton, B.A., R.D. Fetter, and G.W. Davis. 2002. Dynactin is necessary for synapse stabilization. *Neuron*. 34:729–741.

Featherstone, D.E., W.S. Davis, R.R. Dubreuil, and K. Broadie. 2001. *Drosophila* alpha- and beta-spectrin mutations disrupt presynaptic neurotransmitter release. *J. Neurosci.* 21:4215–4224.

Hammarlund, M., W.S. Davis, and E.M. Jorgensen. 2000. Mutations in β-spectrin disrupt axon outgrowth and sarcomere structure. *J. Cell Biol.* 149:931–942.

Hortsch, M., K.L. Paisley, M.Z. Tian, M. Qian, M. Bouley, and R. Chandler. 2002. The axonal localization of large *Drosophila* ankyrin2 protein isoforms is essential for neuronal functionality. *Mol. Cell. Neurosci.* 20:43–55.

Ikeda, Y., K.A. Dick, M.R. Weatherspoon, D. Gincel, K.R. Armbrust, J.C. Dalton, G. Stevanin, A. Durr, C. Zuhlke, K. Burk, et al. 2006. Spectrin mutations cause spinocerebellar ataxia type 5. *Nat. Genet.* 38:184–190.

Jefford, G., and R.R. Dubreuil. 2000. Receptor clustering drives polarized assembly of ankyrin. *J. Biol. Chem.* 275:27726–27732.

Jenkins, S.M., and V. Bennett. 2001. Ankyrin-G coordinates assembly of the spectrin-based membrane skeleton, voltage-gated sodium channels, and L1 CAMs at Purkinje neuron initial segments. *J. Cell Biol.* 155:739–746.

Johnson, K.G., A.P. Tenney, A. Ghose, A.M. Duckworth, M.E. Higashi, K. Parfitt, O. Marcu, T.R. Heslip, J.L. Marsh, T.L. Schwarz, et al. 2006. The HSPGs Syndecan and Dallylike bind the receptor phosphatase LAR and exert distinct effects on synaptic development. *Neuron*. 49:517–531.

Karunanithi, S., L. Marin, K. Wong, and H.L. Atwood. 2002. Quantal size and variation determined by vesicle size in normal and mutant *Drosophila* glutamatergic synapses. *J. Neurosci.* 22:10267–10276.

Kaufmann, N., J. DeProto, R. Ranjan, H. Wan, and D. Van Vactor. 2002. *Drosophila* liprin-alpha and the receptor phosphatase Dlar control synapse morphogenesis. *Neuron*. 34:27–38.

Kittel, R.J., C. Wichmann, T.M. Rasse, W. Fouquet, M. Schmidt, A. Schmid, D.A. Wagh, C. Pawlu, R.R. Kellner, K.I. Willig, et al. 2006. Bruchpilot promotes active zone assembly, Ca2+ channel clustering, and vesicle release. *Science*. 312:1051–1054.

Koh, T.W., P. Verstreken, and H.J. Bellen. 2004. Dap160/intersectin acts as a stabilizing scaffold required for synaptic development and vesicle endocytosis. *Neuron*. 43:193–205.

Komada, M., and P. Soriano. 2002. βIV-spectrin regulates sodium channel clustering through ankyrin-G at axon initial segments and nodes of Ranvier. *J. Cell Biol.* 156:337–348.

Lacas-Gervais, S., J. Guo, N. Strenzke, E. Scarfone, M. Kolpe, M. Jahkel, P. De Camilli, T. Moser, M.N. Rasband, and M. Solimena. 2004. βIVΣ1 spectrin stabilizes the nodes of Ranvier and axon initial segments. *J. Cell Biol.* 166:983–990.

Lee, J.K., R.S. Coyne, R.R. Dubreuil, L.S. Goldstein, and D. Branton. 1993. Cell shape and interaction defects in α-spectrin mutants of *Drosophila melanogaster*. *J. Cell Biol.* 123:1797–1809.

Lee, T., and L. Luo. 1999. Mosaic analysis with a repressible cell marker for studies of gene function in neuronal morphogenesis. *Neuron*. 22:451–461.

Lee, Y.S., and R.W. Carthew. 2003. Making a better RNAi vector for *Drosophila*: use of intron spacers. *Methods*. 30:322–329.

Liu, S.C., L.H. Derick, and J. Palek. 1987. Visualization of the hexagonal lattice in the erythrocyte membrane skeleton. *J. Cell Biol.* 104:527–536.

Marie, B., S.T. Sweeney, K.E. Poskanzer, J. Roos, R.B. Kelly, and G.W. Davis. 2004. Dap160/intersectin scaffolds the periactive zone to achieve high-fidelity endocytosis and normal synaptic growth. *Neuron*. 43:207–219.

Meinertzhagen, I.A., C.K. Govind, B.A. Stewart, J.M. Carter, and H.L. Atwood. 1998. Regulated spacing of synapses and presynaptic active zones at larval neuromuscular junctions in different genotypes of the flies *Drosophila* and *Sarcophaga*. *J. Comp. Neurol.* 393:482–492.

Mohler, P.J., W. Yoon, and V. Bennett. 2004. Ankyrin-B targets beta2-spectrin to an intracellular compartment in neonatal cardiomyocytes. *J. Biol. Chem.* 279:40185–40193.

Moorthy, S., L. Chen, and V. Bennett. 2000. *Caenorhabditis elegans* β-G spectrin is dispensable for establishment of epithelial polarity, but essential for muscular and neuronal function. *J. Cell Biol.* 149:915–930.

Murthy, V.N., T. Schikorski, C.F. Stevens, and Y. Zhu. 2001. Inactivity produces increases in neurotransmitter release and synapse size. *Neuron*. 32:673–682.

Packard, M., E.S. Koo, M. Gorczyca, J. Sharpe, S. Cumberledge, and V. Budnik. 2002. The *Drosophila* Wnt, wingless, provides an essential signal for pre- and postsynaptic differentiation. *Cell*. 111:319–330.

Parnas, D., A.P. Haghighi, R.D. Fetter, S.W. Kim, and C.S. Goodman. 2001. Regulation of postsynaptic structure and protein localization by the Rho-type guanine nucleotide exchange factor dPix. *Neuron*. 32:415–424.

Phillips, G.R., J.K. Huang, Y. Wang, H. Tanaka, L. Shapiro, W. Zhang, W.S. Shan, K. Arndt, M. Frank, R.E. Gordon, et al. 2001. The presynaptic

particle web: ultrastructure, composition, dissolution, and reconstitution. *Neuron*. 32:63–77.

Pielage, J., R.D. Fetter, and G.W. Davis. 2005. Presynaptic spectrin is essential for synapse stabilization. *Curr. Biol.* 15:918–928.

Satzler, K., L.F. Sohl, J.H. Bollmann, J.G. Borst, M. Frotscher, B. Sakmann, and J.H. Lubke. 2002. Three-dimensional reconstruction of a calyx of Held and its postsynaptic principal neuron in the medial nucleus of the trapezoid body. *J. Neurosci.* 22:10567–10579.

Schikorski, T., and C.F. Stevens. 1997. Quantitative ultrastructural analysis of hippocampal excitatory synapses. *J. Neurosci.* 17:5858–5867.

Schikorski, T., and C.F. Stevens. 1999. Quantitative fine-structural analysis of olfactory cortical synapses. *Proc. Natl. Acad. Sci. USA*. 96:4107–4112.

Shen, L., F. Liang, L.D. Walensky, and R.L. Huganir. 2000. Regulation of AMPA receptor GluR1 subunit surface expression by a 4. 1N-linked actin cytoskeletal association. *J. Neurosci.* 20:7932–7940.

Shotton, D.M., B.E. Burke, and D. Branton. 1979. The molecular structure of human erythrocyte spectrin. Biophysical and electron microscopic studies. *J. Mol. Biol.* 131:303–329.

Sweeney, S.T., K. Broadie, J. Keane, H. Niemann, and C.J. O'Kane. 1995. Targeted expression of tetanus toxin light chain in *Drosophila* specifically eliminates synaptic transmission and causes behavioral defects. *Neuron*. 14:341–351.

Thomas, U., E. Kim, S. Kuhlendahl, Y.H. Koh, E.D. Gundelfinger, M. Sheng, C.C. Garner, and V. Budnik. 1997. Synaptic clustering of the cell adhesion molecule fasciclin II by discs-large and its role in the regulation of presynaptic structure. *Neuron*. 19:787–799.

Wagh, D.A., T.M. Rasse, E. Asan, A. Hofbauer, I. Schwenkert, H. Durrbeck, S. Buchner, M.C. Dabauvalle, M. Schmidt, G. Qin, et al. 2006. Bruchpilot, a protein with homology to ELKS/CAST, is required for structural integrity and function of synaptic active zones in *Drosophila*. *Neuron*. 49:833–844.

Wechsler, A., and V.I. Teichberg. 1998. Brain spectrin binding to the NMDA receptor is regulated by phosphorylation, calcium and calmodulin. *EMBO J.* 17:3931–3939.

Wodarz, A., U. Hinz, M. Engelbert, and E. Knust. 1995. Expression of crumbs confers apical character on plasma membrane domains of ectodermal epithelia of *Drosophila*. *Cell*. 82:67–76.

Zhen, M., and Y. Jin. 1999. The liprin protein SYD-2 regulates the differentiation of presynaptic termini in *C. elegans*. *Nature*. 401:371–375.

Zito, K., R.D. Fetter, C.S. Goodman, and E.Y. Isacoff. 1997. Synaptic clustering of Fascilin II and Shaker: essential targeting sequences and role of Dlg. *Neuron*. 19:1007–1016.